PLASMA-POLYMERIZED C$_{60}$ FILMS

M. Ramm[1], M. Ata[1], Th. Gross[2] and W. Unger[2]

[1] Sony Corporation Frontier Science Laboratories, 2-1-1, Shinsakuragaoka, Hodogaya-ku,
Yokohama 240-0036, Japan
[2] Bundesanstalt für Materialforschung und –prüfung, Unter den Eichen 44-46 D-12203 Berlin, Germany

Abstract. We studied the polymerization of C$_{60}$ under different Ar plasma conditions. Films were either deposited in the pressure range between 1.3 and 40 Pa applying input power of 50 W or evaporated C$_{60}$ films were exposed to Ar plasma of 30 and 50 W. The films were investigated by Raman spectroscopy, X-ray photoelectron spectroscopy (XPS) and carbon *K* near-edge X-ray-absorption fine structure spectroscopy (NEXAFS). The films were non-uniform and consisted of unpolymerized C$_{60}$, dimers, linear chains and polymeric planes. In comparison with evaporated C$_{60}$ the XPS C 1s peak is broader and asymmetric for the C$_{60}$ polymer and its shake-up satellites diminished. Furthermore, the features of the valence band as well as the features of the π^* antibonding orbitals of the C$_{60}$ polymer are broader and reduced in intensity.

1. INTRODUCTION

The 30 double bonds of the fullerene C$_{60}$ provide numerous sites for intermolecular attachment to form new polymeric C$_{60}$ phases. The observation of polymerization was first reported for photo-induced C$_{60}$ [1]. Other polymerization routes include the application of hydrostatic pressure [2], charge transfer from alkali-metal dopants to C$_{60}$ molecules [3,4], plasma [5] and the electrochemical process [6]. A [2+2] cycloaddition via electronically excited triplet states is considered the most likely pathway of the polymerization in the photopolymer [1] and the high-pressure/high-temperature- (HPHT) induced polymer [7]. Intensive investigations of photo-polymerized C$_{60}$ have been performed [1,8,9,10] but the detailed structure of photo-polymerized C$_{60}$ is not well known. The various structures of the pressure polymerized and the alkali-metal doped C$_{60}$ are on the other hand relatively well known [2,3,7-9,11,12].

We applied radio-frequency (rf) plasma to polymerize C$_{60}$ and studied the polymerization using Raman spectroscopy, core level and valence band X-ray photoelectron spectroscopy (XPS) and carbon *K* near-edge X-ray-absorption fine structure spectroscopy. Raman spectroscopy has been widely used to characterize fullerene polymers. The original Raman active modes of C$_{60}$ split and shift and new modes are generated due to the lowering of the I$_h$ molecular symmetry as result of the formation of covalent bonds between the fullerene molecules in the polymer [13]. Near-edge X-ray-absorption fine structure spectroscopy (NEXAFS) has proven to be especially useful in examining the electronic structure of carbon materials because it provides structural information about the π^* and σ^* antibonding orbitals and distinguishes between sp^2 and sp^3 bonding [14,15].

2. EXPERIMENTAL DETAILS

Films 500-nm thick were deposited in a parallel-plate radio frequency reactor operating at 13.56 MHz by sublimation of C$_{60}$ powder (purity > 99.2 %) in Ar plasma on silicon substrates. The films were deposited at gas pressures of 1.3, 3.3, 6.7, 13, 20, 26.7 and 40 Pa by applying 50 W input power. At 6.7·10^{-4} Pa evaporated 200-nm thick C$_{60}$ films were exposed to Ar plasma of 30 and 50 W for 4 hours and 30 minutes, respectively.

Raman spectra were recorded using a 514.5 nm Ar$^+$ laser as excitation source and a Jobin Yvon

---

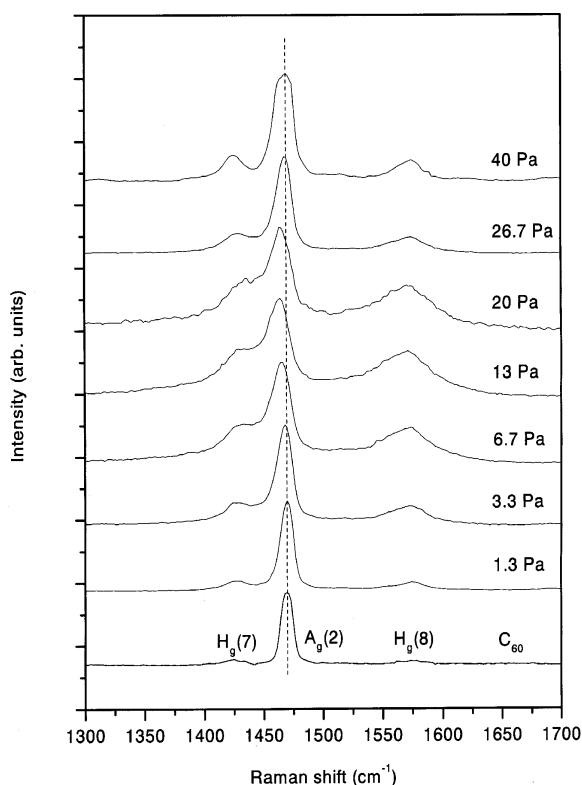Corresponding author: M. Ramm, e-mail: Matthias.Ramm@jp.sony.com

Fig. 1. Raman spectra between 1300 and 1700 cm^{-1} of films deposited at different pressure.

Fig. 2. Intensities of the components in the vicinity of the pentagonal pinch mode.

—■— 1469 cm^{-1}
—●— 1464 cm^{-1}
—▲— 1459 cm^{-1}
—▼— 1446 cm^{-1}
—◆— 1434 cm^{-1}
—+— 1424 cm^{-1}
—×— 1406 cm^{-1}
—*— 1370 cm^{-1}

spectrometer equipped with a nitrogen-cooled CCD detector. The applied power was reduced below 4 mW to avoid photo-induced transformation during the course of the investigation.

Valence band and core level spectra were obtained employing a SSX 100 photoelectron spectrometer. We used monochromatized Al K_α radiation, a fixed energy pass at 50 eV and a take-off angle of 55° *vs.* surface normal.

NEXAFS spectroscopy was carried out at the HE-TGM 2 monochromator beam line #33.12 of the BESSY synchrotron light source (Berlin, Germany) [16]. Spectra were acquired at the C *K*-edge in the partial electron yield mode (PEY).

3. RESULTS AND DISCUSSION

The Raman spectrum of C$_{60}$ shows only 10 active modes. The high-frequency A_g pentagonal pinch mode observed at 1469 cm^{-1} is the most intensive as well as the most sensitive in probing the polymerization state [2,17].

Fig. 1 shows the Raman spectra between 1300 and 1700 cm^{-1} of the deposited films. The region of the pentagonal pinch mode is different for each of the spectra. Line-shape analyses were performed
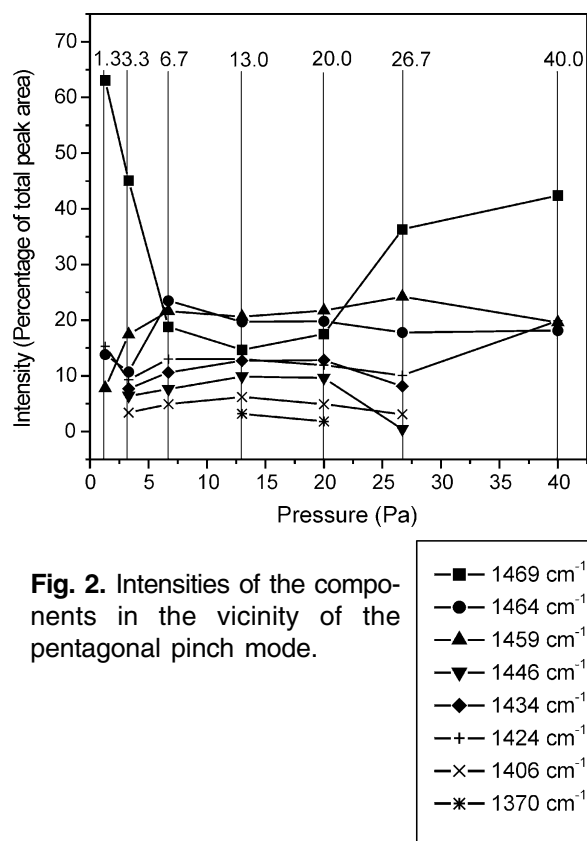
resolving the peaks in the vicinity of the pentagonal pinch mode to get more structural information. Voigt line shapes were fitted using a peak-fitting program. The center frequencies for the different contributions were observed very nearly at the same frequency, and are ~1406, ~1424, ~1434, ~1446, ~1459, ~1464 and 1469 cm^{-1}. However, looking at the positions and relative intensities of the components, we find differences because of the varying pressure, as shown in Fig. 2. The modes representing polymeric planes at ~1406 [8,12], ~1434 [8,9] and ~1446 cm^{-1} [8,12] are absent for the depositions at 1.3 and 40 Pa. Only dimers and linear chains were formed under these conditions, as can be seen in the modes at ~1464 [10,17,18] and ~1460 cm^{-1} [10,17], respectively. Despite the different deposition conditions, all films contained unpolymerized C$_{60}$, as is seen by the presence of the mode at ~1469 cm^{-1}. The amount of unpolymerized C$_{60}$ ranges from 63.1 (1.3 Pa) to 14.7 % (13 Pa). The films deposited in the range from 6.7 to 26.7 Pa contain roughly an equal amount of dimers and linear chains. The ratio of dimers to longer chains deposited at 6.7, 13 and 20 Pa is approximately 1:1. Polymeric planes were formed predominately under these conditions in larger amounts. The line-shape analyses of plasma
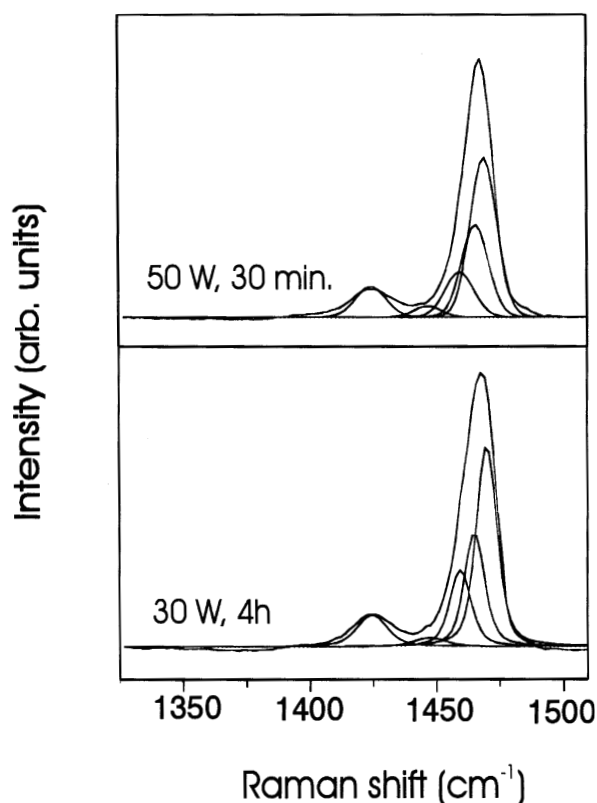
Fig. 3. Raman spectra indicating the different components in the vicinity of the pentagonal pinch mode for plasma treated films.

Fig. 4. XPS C 1s spectra of C_{60} and C_{60} plasma polymer.

treated films are shown in Fig. 3. Dimers and linear chains were formed predominately under the specified conditions in larger amounts. According the mode at ~1446 cm^{-1} only small contributions of polymeric planes are present. The modes in the vicinity of the pentagonal pinch mode can be assigned to well-defined polymeric species for the films except the mode ~1370 cm^{-1}.

It cannot be ruled out that plasma-deposited C_{60} polymer films contain amorphous carbon due to the decomposition of the C_{60} cage. Two broad features centered approximately at 1360 and 1620 cm^{-1} appear in the Raman spectra of amorphous carbon [19]. The line-shape analyses reveal a mode located at ~ 1370 cm^{-1} in the spectra of the films deposited at 13 and 20 Pa, suggesting the incorporation of small amounts of amorphous carbon.

The XPS C 1s peaks of both evaporated C_{60} and of the film deposited at 13 Pa are shown in Fig. 4. The FWHM of the C 1s peak of the plasma-deposited film increased by 0.5 eV to 1.3 eV compared to the FWHM of 0.8 eV of the evaporated C_{60} film. Moreover, the shape of the C 1s peak becomes asymmetric in the direction of higher binding energy. The calculated chemical shifts of the C 1s
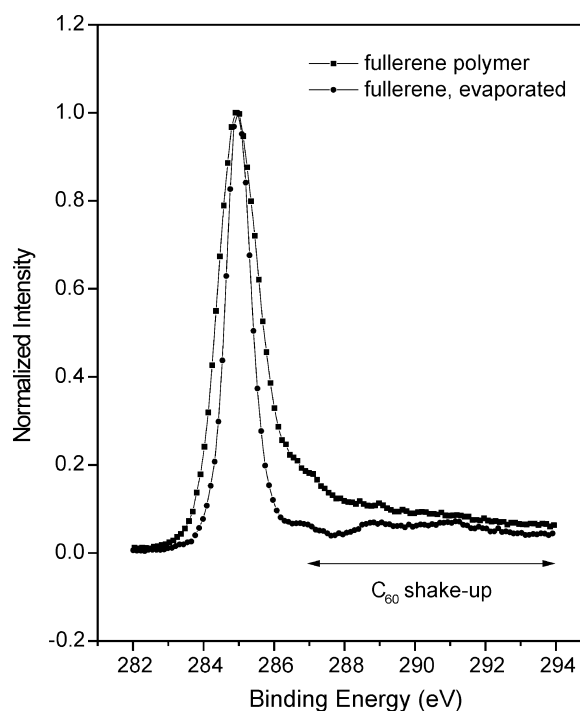
binding energy of +0.3 eV per four-membered ring in C_{60} polymers with respect to the isolated C_{60} molecule [20] can only partially explain the broadening. On the other hand, we found 9 at.% oxygen by XPS. The high overall FWHM and the broad tail in the direction of higher binding energy indicate that contributions of a variety of different carbon species such as C-O, C-O-O and C=O are superimposed by shake-up features. Therefore, both polymerization and oxidation cause the broadening of the C 1s peak of the plasma-deposited film. Fig. 5 shows the XPS valence band spectra. It is clear that the peaks of the plasma-deposited film become broader and reduced in intensity. In addition to the carbon states, the O 2s peak appears at about 27 eV. UPS [21,22] and XPS [23] investigations showed that additional features appear in the valence band and the structures become broadened and reduced in amplitude upon photopolymerization. Theoretical investigations of different polymeric phases of C_{60} [24] indicate that the relatively strong changes in the valence band of the plasma-deposited film are mainly due to the polymerization to higher polymers. Oxidation and the occurrence of fragmented fullerene and amorphous carbon species may provide additional contributions to the valance band spectrum.

The unoccupied bands observed by C K near-edge X-ray absorption fine structure spectroscopy are illustrated in Fig. 6. A number of characteristic
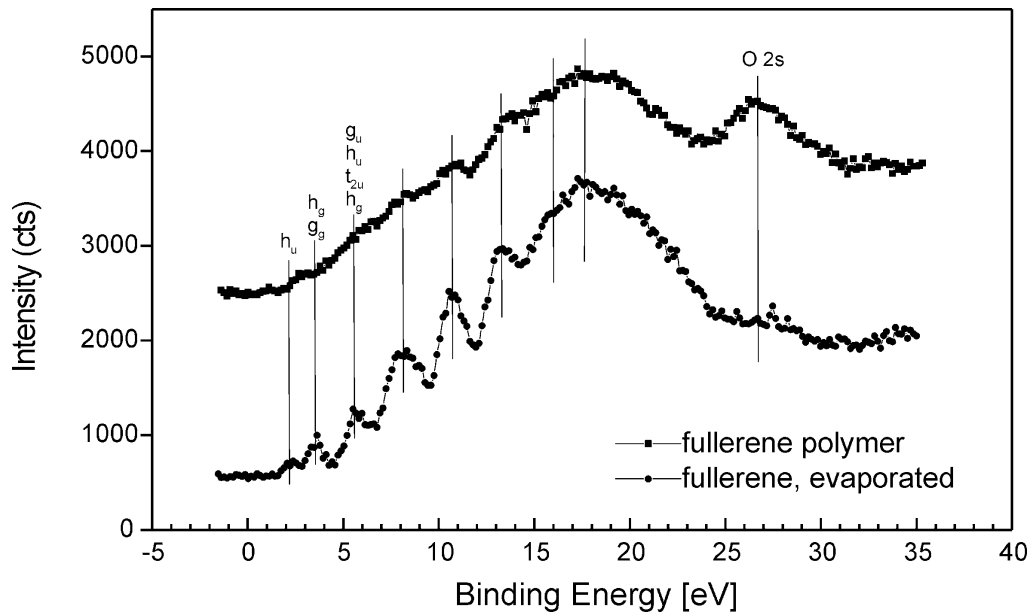
Fig. 5. XPS valence band region of C_{60} and C_{60} plasma polymer.

resonant π^* features were observed between 284 and 291 eV for C_{60} [25]. The π^* resonances of the plasma-deposited film become broader and those at 286.2 and 288.5 eV are significantly reduced in intensity in comparison to evaporated C_{60}.

4. SUMMARY

C_{60} was polymerized under different Ar plasma conditions. Films were either deposited in the pressure range between 1.3 and 40 Pa applying input power

of 50 W or evaporated C_{60} films were exposed to Ar plasma of 30 and 50 W. The films were investigated using Raman spectroscopy, XPS and NEXAFS. Detailed structural information was derived from line-shape analyses resolving the peaks in the vicinity of the pentagonal pinch mode. The films have a non-uniform film composition and contain unpolymerized C_{60}, dimers, linear chains and polymeric planes. Amorphous carbon was found in films deposited at certain conditions. In contrast to C_{60}, we found a
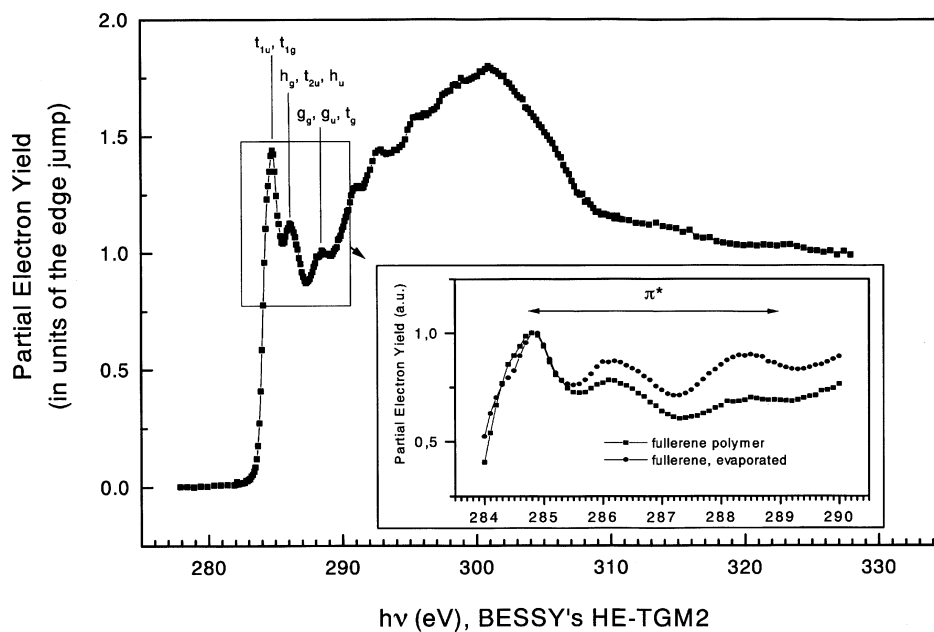

Fig. 6. C *K*-edge of the C_{60} plasma polymer. The insert shows the expanded π^*-region of C_{60} and C_{60} plasma polymer.

broadened, asymmetric C 1s peak, strongly diminished features in the valence band, as well as broadened and intensity-reduced π^* antibonding orbital resonances. Although the contribution of oxidation and the formation of amorphous carbon must be accounted for, the primary changes in the XPS and NEXAFS spectra clearly resulted from polymerization.

REFERENCES

[1] A. M. Rao, P. Zhou, K. Wang, G. T. Hager, J. M. Holden, Y. Wang, W. Lee, X. Bi, P. C. Eklund, D. S. Cornett, M. A. Duncan and I. J. Amster // *Science* **259** (1993) 955.

[2] Y. Iwasa, T. Arima, R. M. Fleming, T. Siegrist, O. Zhou, R. C. Haddon, L. J. Rothberg, K. B. Lysons, L. Carter, A. F. Hebard, R. Tycko, G. Dabbagh, J. J. Krajewski, G. A. Thomas and T. Yagi // *Science* **264** (1994) 1570.

[3] P. W. Stephens, G. Bortel, G. Faigel, M. Tegze, A. Janossy, S. Pekker, G. Oszlanyi and L. Forro // *Nature* **370** (1994) 636.

[4] J. Winter and H. Kuzmany // *Solid State Commun.* **83** (1992) 1321.

[5] N. Takahashi, H. Dock, N. Matsuzawa and M. Ata // *J. Appl. Phys.* **74** (1993) 5790.

[6] P. Strasser and M. Ata // *J. Phys. Chem. B* (1998) 4131.

[7] M. Nunez-Regueiro, L. Marques, J.-L. Hodeau, O. Bethoux and M. Perroux // *Phys. Rev. Lett.* **74** (1995) 278.

[8] A. M. Rao, P. C. Eklund, J.-L. Hodeau, L. Marques and M. Nunez-Regueiro // *Phys. Rev. B* **55** (1997) 4766.

[9] T. Wagberg, P. Jacobsson and B. Sundqvist // *Phys. Rev. B* **60** (1999) 4535.

[10] B. Burger, J. Winter and H. Kuzmany // *Z. Phys. B* **101** (1996) 227.

[11] G. Oszlanyi and L. Forro // *Solid State Commun.* **93** (1995) 265.

[12] V. A. Davydow, L. S. Kashevarova, A. V. Rakhmanina, V. Agafonov, H. Allouchi, R. Ceolin, A. V. Dzyabchenko, V. M.

Senyavin and H. Szwarc // *Phys. Rev. B* **58** (1998) 14786.

[13] For a comprehens. review: M. S. Dresselhaus, G. Dresselhaus and P. C. Eklund // *J. Raman Spec.* **27** (1996) 351.

[14] D. Wesner, S. Krummacher, R. Carr, T. K. Sham, M. Strongin, W. Eberhardt, S. L. Weng, G. Williams, M. Howells, F. Kampas, S. Heald and F. W. Smith // *Phys. Rev.* **28** (1983) 2152.

[15] D. M. Gruen, A. R. Krauss, C. D. Zuiker, R. Csencsits, L. J. Terminello, J. A. Carlisle, I. Jimenez, D. G. J. Sutherland, D. K. Skuh, W. Tong and F. J. Himpsel // *Appl. Phys. Lett.* **68** (1996) 1640.

[16] *Research at BESSY. A User's Handbook,* ed. by Ch. Jung (BESSY 1993).

[17] P. C. Eklund, P. Zhou, K.-A. Wang, G. Dresselhaus and M. S. Dresselhaus // *J. Phys. Chem. Solids* **53** (1992) 1391.

[18] S. Lebedkin, A. Gromov, S. Giesa, R. Gleiter, B. Renker, H. Rietschel and W. Krätschmer // *Chem. Phys. Lett.* **285** (1998) 210.

[19] P. Lespade, R. Al-Jishi and M. S. Dresselhaus // *Carbon* **20** (1982) 427.

[20] D. Porzag, M. R. Pederson, Th . Frauenheim and Th. Köhler // *Phys. Rev. B* **52** (1995) 14963.

[21] B. S. Itchkawitz, J. P. Long, T. Schedel-Niedrig, M. N. Kabler, A. M. Bradshaw, R. Schlögl and W. R. Hunter // *Chem. Phys. Lett.* **243** (1995) 211.

[22] G. P. Lopinski, J. R. Fox and J. S. Lannin // *Chem. Phys. Lett.* **239** (1995) 107.

[23 J. Onoe, A. Nakao and K. Takeuchi // *Phys. Rev. B* **55** (1997) 10051.

[24] J. Schulte, M. C. Böhm, T. Schedel-Niedrig and R. Schlögl // *Ber. Bunsenges. Phys. Chem.* **101** (1997) 1531.

[25] L. J. Terminello, D. K. Shuh, F. J. Himpsel, D. A. Lapiano-Smith, J. Stöhr, D. S. Bethune and G. Meijer // *Chem. Phys. Lett.* **182** (1991) 491.